J. Earth Syst. Sci. (2020)129 68
https://doi.org/10.1007/s12040-019-1336-x

Deep insight to the complex aquifer and its characteristics from high resolution electrical resistivity tomography and borehole studies for groundwater exploration and development

Dewashish Kumar*, Setbandhu Mondal and Taufique Warsi

CSIR–National Geophysical Research Institute, Hyderabad 500 007, India.
**Corresponding author. e-mail: dewashishkumar@ngri.res.in*

MS received 26 April 2019; revised 14 November 2019; accepted 15 November 2019

Discovering and locating the source and availability of groundwater in a plateau region of Chhotanagpur gneissic complex, where there is a varied hydrogeological characteristics, is a crucial task for earth scientists. One such region located at Garh Khatanga near Ranchi, Jharkhand, India was closely studied for groundwater assessment and exploration. High resolution electrical resistivity tomography 2D data were acquired to probe deep inside the earth up to a maximum depth of 220 m using state-of-the-art electrical resistivity tomography technique and mapped geoelectrical subsurface images at 16 sites in three different blocks along a 7.2 km line for prospecting and exploration of groundwater resources. The geophysical inversion of the 2D resistivity data revealed prospect groundwater scenario at six sites based on the hydrogeological interpretation and the significant resistivity contrast between the highly weathered/fractured and the massive rocks. The modelled resistivity sections revealed different degree of weathered, fractured and saturated weathered/fractured strata as well as clearly indicated the presence of a totally hard massive rock within the subsurface lying between ∼30 and 220 m depths. The geophysical anomalies were confirmed and validated by borehole drilling at four sites up to a maximum depth of 215 m with yields ranging from 2.0 to 4.25 inch, which is equivalent to 5632–63769 l/hr of groundwater exploitation. These yields of groundwater resources are rated as good aquifer(s) in the plateau region of Chhotanagpur gneissic complex. The characteristics resistivity for fracture zone varies from 140 to 1300 Ωm, while for saturated weathered/fractured it ranges from 10 to 1000 Ωm. On joint interpretation of the 2D resistivity models and the borehole lithology data, it clearly shows the average resistivity of the aquifer zone lies in the range 50–500 Ωm. The present study along with the conceptual geological models provided a sound knowledge of hard rock hydrogeology in the plateau region with complex geological settings and these helped to achieve significant results for groundwater exploration and development of the resources of the studied area as well as take up such challenging work in exploring the prospect groundwater resources in other similar geological setting of the country.

Keywords. 2D resistivity tomography; plateau region; Chhotanagpur gneissic complex; deeper groundwater resource; Jharkhand, India.

Published online: 10 February 2020

1. Introduction

Groundwater is the only source of subsurface fresh water that is used by human being throughout the country as well as globally. The amount and availability of groundwater varies from one type of geological formation and structure to another. The maximum it is available in the alluvium region and the least in the hard rock aquifers system. In hard rock regions, there is a large scale of variability of groundwater, which depends on the type of terrain, extent of fracturing and fissuring within the rock mass, existence of a secondary porosity as well as the connectivity of fracture(s) to the recharge source area. In a plateau region, it is again a very difficult problem to delineate the location of groundwater availability within the subsurface. However, groundwater prospecting in a hard rock terrain is a difficult task due to its typical and varied hydrological properties of unconfined, confined and fractured aquifer system. Hydrogeologically hard rocks are those lithological units, which lack the primary porosity. However, the network of horizontal, vertical joints and the fracture(s) within the rock strata makes it the aquifer system, provided it should be connected to the rainfall recharge source. Electrical resistivity method is the cheapest and the most reliable method due to wide range of resistivity values, which covers almost the entire geological formations within the subsurface. Electrical resistivity study assumes and merits a special significance for mapping aquifers in hard rock areas in different geological settings. A two-dimensional (2D) resistivity survey of Chikotra basin, southern part of Kolhapur district in the Deccan Volcanic Province of Maharashtra was accomplished by Gupta *et al.* (2015) for delineation of aquifer. Their results from the 2D inverted models depicting resistivity variation with depths, suggest the occurrence of aquifer(s) mostly in weathered/fractured zones within the traps or beneath it. Radhakrishna (1952, 1993) has described the evolution of Mysore Plateau, its structural and physiographic evolution. The first high-resolution electrical images of the High Agri Valley, a fault-bounded basin representing one of the most active fault systems in southern Italy, has been studied by Colella *et al.* (2004). The electrical images give several information about the depth and complex structure of the High Agri basin up to 500 m, supplying a considerable contribution to its geological interpretations. Kumar *et al.* (2016b) studied the granitic hard rock aquifer and clearly mapped weathered, highly weathered granite as well as the massive granite, which are seen from true resistivity values of the modelled dataset and the resistivity ranges from ∼10 to 28,300 Ωm up to 131 m depth. The results from the resistivity models convey that the prospect groundwater zone(s) are only visible at the deeper depths (Kumar *et al.* 2016b).

In the present context, a typical hard rock region in a plateau region of Chhotanagpur gneissic complex (CGC) had been studied for groundwater assessment, exploration and prospecting. Based on the reconnaissance survey in the area of study at the new campus at IIAB, Ranchi Jharkhand, a detailed scientific work was undertaken to understand the plateau region and its geological setting in order to delineate and demarcate the potential target(s) zones for groundwater exploration and development of the resources. The main objective of the work is mapping and delineation of groundwater prospect zones at shallow as well the deeper depths. In the first phase of study 16 2D electrical resistivity tomography (ERT) survey was conducted in an area of about 122 acres in the month of June–July, 2015 for detailed mapping of the subsurface lithological formations and geological structure for identifying suitable and prospect sites for deep drilling up to the maximum depth of 200 m in and around the study area. In the 2nd phase of work, the groundwater potential zones were delineated at six sites based on the hydrogeological interpretation from the results of the 2D resistivity modelled dataset, which covered three blocks – A, B and D of the study area. The borehole drilling was accomplished at four anomalous sites based on the hydrogeological interpretation for groundwater exploitation and development.

2. Study area

The study area is about 122 acres of the Indian Institute of Agricultural Biotechnology (IIAB), Namkum Ranchi, a unit of Indian Council of Agricultural Research (ICAR), New Delhi at Ghar Khatanga area near Ranchi, Jharkhand, India. It comprises of open land with a number of small and big tress, fallow pasture, rainfed land and is a part of agricultural area. It is located at a distance of about 15 km away from the main town Ranchi near the highway close to ring road in the north direction. It lies between latitudes 23°15′44.70″–23°16′30.0″N and longitudes 85°20′14.70″–85°20′58.30″E (figure 1). The study area is more or less flat with no major geological structure outcrop and features seen on the

surface. The soil is light brown laterite type and its thickness is less than 20 m within the area of study. The subsurface constitute weathered rock up to 25–30 m depth, at the deeper depths lies the weathered/fractured and the massive hard rock. Ranchi district experiences subtropical climate, which is characterized by hot summer from March to May and well distributed rainfall during southwest monsoon from June to October in a year. While the rain scenario during the period June–July 2015 (beginning of monsoon) was low. In fact, it rained one day with low rainfall for a short time during the survey period, which hardly influences resistivity of the top soil, weathered layer and subsurface deeper rock strata. The winter season in the area is marked by dry and cold weather during the months of November–February in a year. The normal annual rainfall in and around the study area is 1100 mm. Maximum rainfall has been observed from June to October months. About 90% of the total annual rainfall is received in the monsoon period. The northernmost and southernmost parts of the district are covered with hillocks and forests. The study area falls in the southern part of Ranchi district with an altitude variation of 650–662 m above mean sea level. It is a part of Chhotanagpur plateau (Singh 2013).

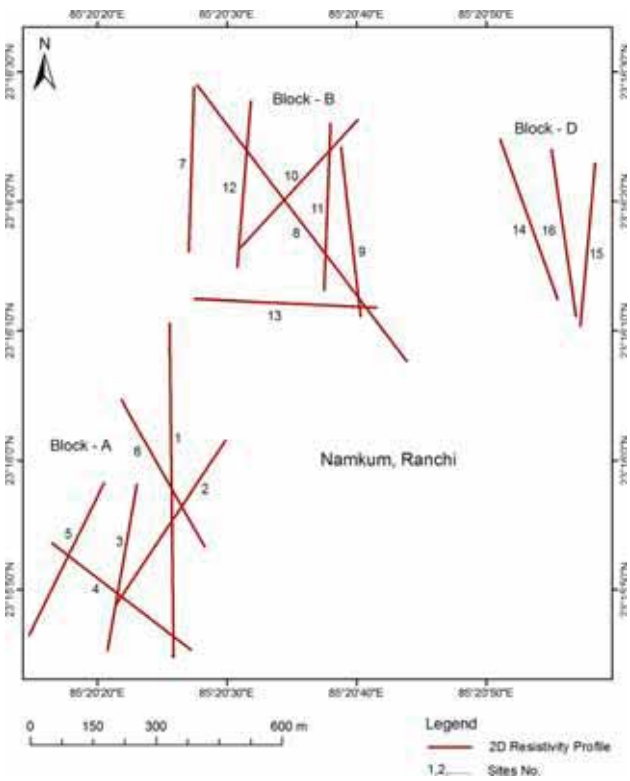

Figure 1. Map showing the geographical location and 2D resistivity profiles in block A, B and D in the study area.

3. Geology and hydrogeology of area

The Ranchi district is having a varied hydrogeological characteristics due to which groundwater potential differs from one region to another. It is underlain by Chhotanagpur granite-gneiss of pre-Cambrian age in three-fourth part of the district (Singh 2013). The main geology of the study area is CGC as well as the basic rocks. The geological map of the area is shown in figure 2. It is a part of Indian peninsular shield – a stable cratonic block of the earth crust. The Chhotanagpur plateau represents a vast area from western part of Bihar to the border of West Bengal in the east. Physiographically, the plateau has been divided into two parts, namely, Ranchi plateau and plateau. The Ranchi plateau has a flat to undulating topography with occasional ridges. It gradually slopes down towards SE in the hilly regions of Singhbhum. The most important lithological unit comprises archaean metamorphites with associated intrusives and sediments belonging to Gondwana Supergroup and their associated rocks (Singh and Verma 2015). Two types of aquifers are found in and around Ranchi, namely, the weathered and the fractured aquifers system. The thickness of weathered aquifers varies from 10 to 25 m in a granite terrain and 30–60 m in a lateritic terrain. In the weathered aquifer, groundwater occurs in an unconfined condition while in fractured and fissured part of the aquifers groundwater occurs in semi-confined to confined condition (Singh 2013), which is at deeper depths. The hydrogeological investigation was carried out in and around the study area in order to know the general water table scenario and its variability as well as the availability of groundwater in and around the area of study. The water level was measured from five open large diameter dugwells including one borewell. It was found that the static water levels vary from 5.25 to 8.05 m below ground level (bgl). This suggests the water table in and around the study area is shallow. There is a clear-cut indication of substantial rainfall recharge to the water table, which is reflected in terms of shallow to medium water levels in and around the study area.

4. Materials and methods

4.1 *High resolution geophysical investigations: Electrical resistivity tomography*

Two-dimensional ERT is an active source geophysical method to probe into the earth to better understand the subsurface resistivity and conductivity changes as

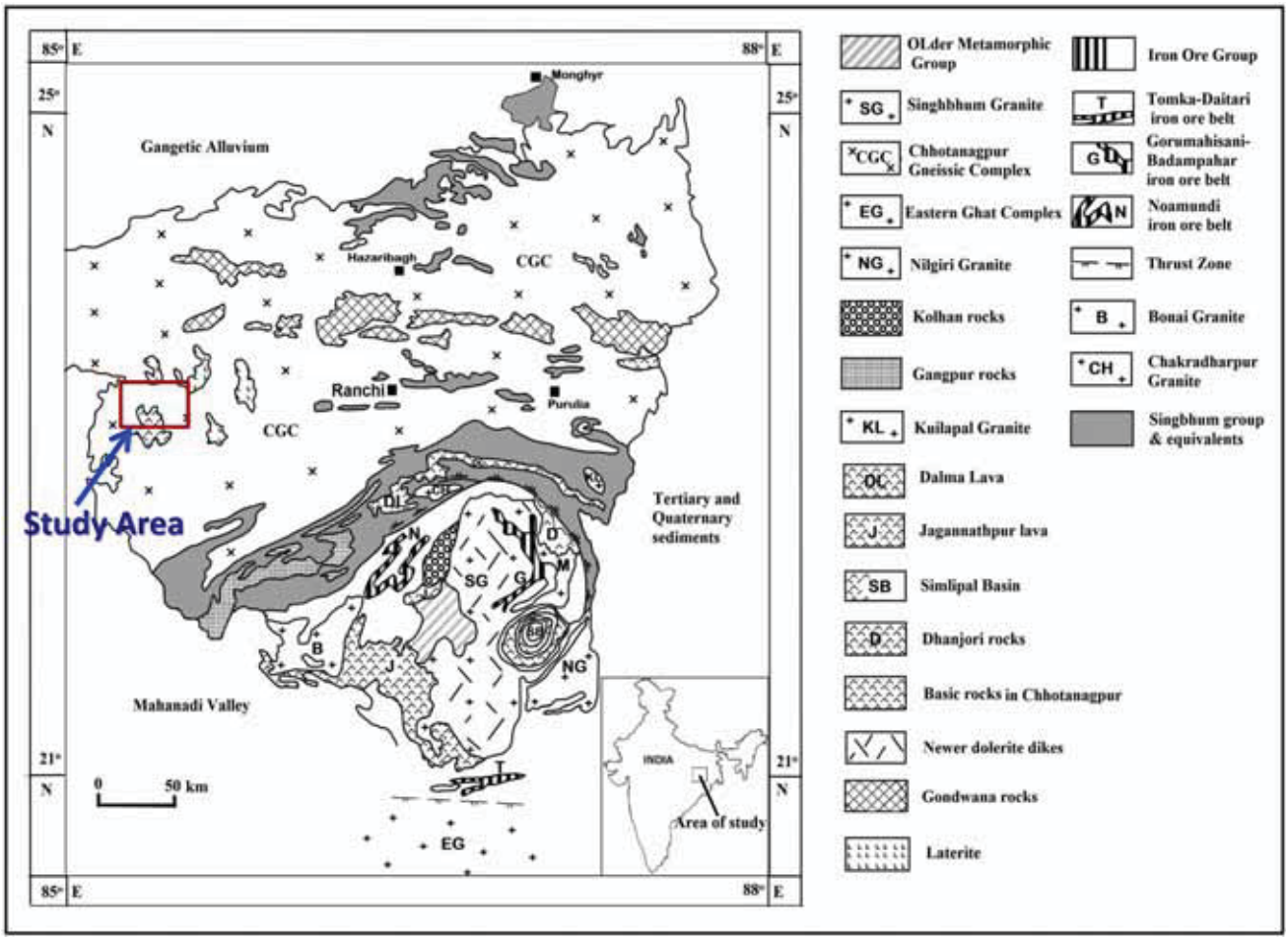

Figure 2. Detailed geological map of the East Indian Shield (after Baidya 2015) showing the study area with inset map of India.

well as variations of the rock materials and their property with depths. It is extensively used in many geoscientific studies particularly in environmental, mineral prospecting and groundwater exploration and prospecting (Griffiths *et al.* 1990; Griffiths and Barker 1993; Dahlin 1996; Hossain 2000; Suzuki *et al.* 2000; Batayneh Awni 2001; Steeples 2001; Demanet *et al.* 2001; Kumar 2004, 2012; Adepelumi *et al.* 2006; Kumar *et al.* 2010, 2014, 2016a, 2017; Andrade 2011; Robert *et al.* 2011; Thiagarajan *et al.* 2018). The high resolution electrical resistivity full waveform sampling and recording of the dataset namely, resistivity (ABEM 2012) with eight windows timing set up and equal duration for current-on and current-off in the measurement cycle were acquired at 16 sites covering 7.2 km line (figure 1). We deployed gradient as well as pole–dipole arrays for the complete, necessary set of data acquisition and the required relevant information for detailed mapping of the subsurface geological strata. The advantage of the pole–dipole configuration is that it offers a good resolution of geological structures as well as gives a larger depth penetration within a limited electrode spread (Loke 2012b) and a relatively good horizontal coverage on the ground. This array has significantly a higher signal strength compared to a dipole–dipole array. But it requires a remote electrode, the current (C2) electrode, which must be placed at far off distance away from the survey line. At the same time, the pole–dipole array is less affected by the C2 remote electrode compared to the pole–pole array (Loke 2012b). In the present survey, a total of 1040–1329 apparent resistivity full waveform data points were collected for each site by planting either 41 or 81 electrodes, respectively, depending on the availability of space in the field area. The maximum electrode spacing used in the survey was 10 m and all these electrodes were planted at one stretch, minimum 10–15 cm vertically below the surface in a multi-electrode mode for a complete data acquisition set for each of the 16 sites using state-of-the-art 4 channel ABEM Terrameter LS system (ABEM 2012). In the present survey, we used gradient array only at

site-1 and at the rest of the sites 2–16 pole–dipole array was successfully laid due to constrain in the availability of space and to achieve the target depth of interest in the area. The pole–dipole array is well suited for multichannel data acquisition system and for larger depth penetration within the subsurface lithology. The measured apparent resistivity 2D datasets were first analyzed and later processed for eliminating any noisy or bad data points in the gathered dataset. These apparent field datasets do contain anomalies of the subsurface body and is clearly reflected and viewed from the 2D pseudosections at different sites with depths. The measured field datasets are presented in the form of pseudosections with dense sampling of apparent resistivity measurements at shallow depth (Loke 1997, 2012a) with a vast coverage both in lateral and vertical directions with respect to the ground level. Thereafter, the processed and filtered dataset was inverted using least squares inverse approach with smoothness constrained (Sasaki 1992; Loke 1997, 2012a) and with a standard Gauss–Newton optimization technique by the help of recent version of RES2DINV inversion code. In the 2D inversion of resistivity data, Dahlin and Loke (1998) have found that in areas with a large resistivity contrasts the Gauss–Newton least-squares inversion method leads to significantly more accurate results than the quasi-Newton method (Loke and Barker 1996; Loke and Dahlin 2002). This actually reproduces a realistic subsurface 2D inverted resistivity models with depth both in the lateral and vertical directions. These 2D inverted models of the subsurface geology presented in the form of true resistivity revealed the geological layers, structures and hydrogeological features based on the resistivity contrast and the anomalous zone(s) with respect to the host rock. These 2D resistivity models ultimately interpreted in terms of different rock layers and their property as well as mainly in terms of hydrogeological importance (Kumar 2012; Kumar *et al.* 2015, 2016a; Thiagarajan *et al.* 2018) for groundwater exploration and development in this particular geological setting.

5. Results

5.1 *Interpretation of 2D electrical resistivity tomography models*

5.1.1 *Site-1 (Block-A)*

The 2D inverted resistivity model at site-1 in block-A is laid in N–S direction covering a lateral distance of 800 m in length using gradient array and deploying 81 electrodes with a maximum 10 m electrode spacing on the ground. The resistivity model shows a large resistivity contrast with a resistivity range of ∼15 to >250,000 Ωm. It shows a highly weathered rock in the northern side at a lateral distance between 210 and 220 m and depicts a very low resistivity zone <100 Ωm, which is extending up to a depth of 131 m and beyond the model depth. This particular low resistivity zone between <100 and 250 Ωm from near surface layer to 131 m depth is a potential target for groundwater exploration and development (figure 3). All along the 2D section from this very low resistivity zone and towards the southern side, it shows a much higher resistivity of the subsurface geological formation with no prospect groundwater zone (figure 3).

5.1.2 *Site-5 (Block-A)*

The 2D inverted resistivity model at site-5 is laid in N–S direction as shown in figure 4. It shows a low resistivity <200 Ωm from near surface layer to a depth of 25 m and a heterogeneous subsurface scenario as well as high resistivity in the northern side of the section but as we move from the centre to the southern side there is a decrease in resistivity – a potential groundwater zone is delineated, which is bounded above and below by the high resistivity zone at a depth between 70 and 85 m and within the lateral distance 240–320 m towards south (figure 4). This prospect groundwater zone is the potential target for groundwater exploration and it appears to extend in SW direction as revealed from the model resistivity section (figure 4). Below this potential groundwater zone lies the high resistivity rock at the deepest depth of investigation.

5.1.3 *Site-7 (Block-B)*

The 2D inverted resistivity model at site-7 in block-B is laid in S–N direction (figure 5). It shows a low resistivity <100 Ωm at and nearby the surface and up to a depth of 20 m followed by an increase in resistivity with depths. The northern side of the resistivity section shows more prospects for groundwater exploration as compared to the southern side (figure 5). It revealed a low resistivity formation between 300 and 550 Ωm from 27 to 110 m depth in northern side and is connected to the near surface layers whose resistivity < 100 Ωm,

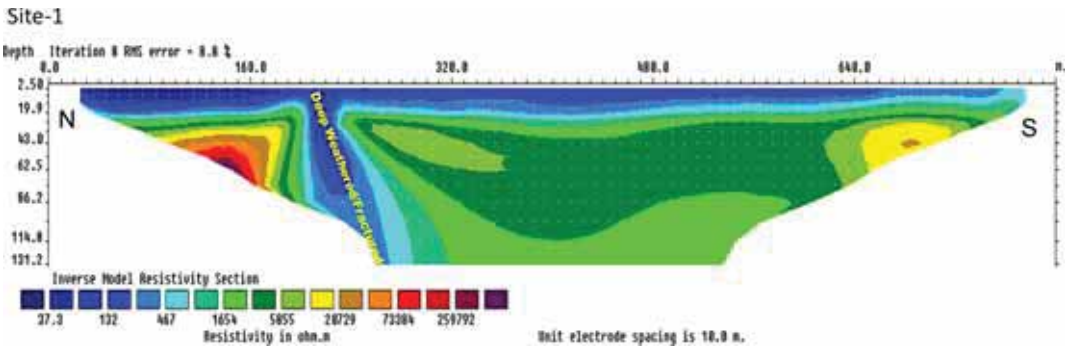

Figure 3. 2D inverted resistivity model with large resistivity contrast showing the prospect groundwater zone towards the northern side of the resistivity section at site no. 1.

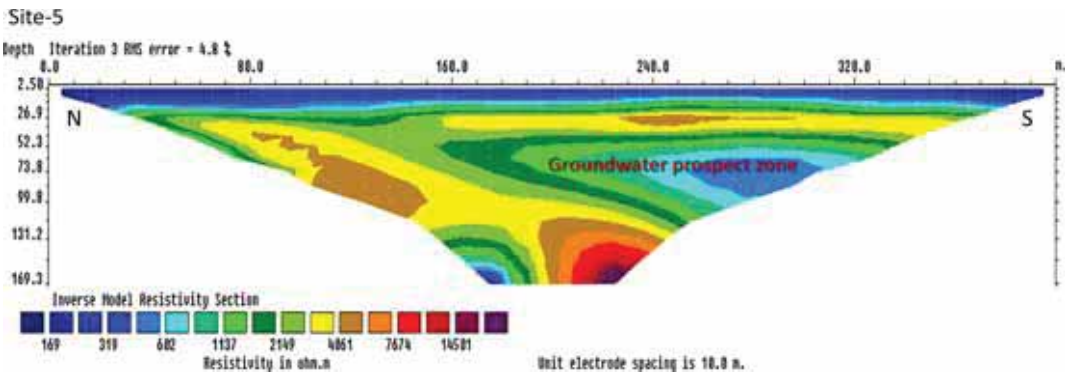

Figure 4. The figure depicts the 2D inverted resistivity model showing heterogeneous subsurface, high resistivity as well as groundwater prospect zone towards south of the section at site no. 5.

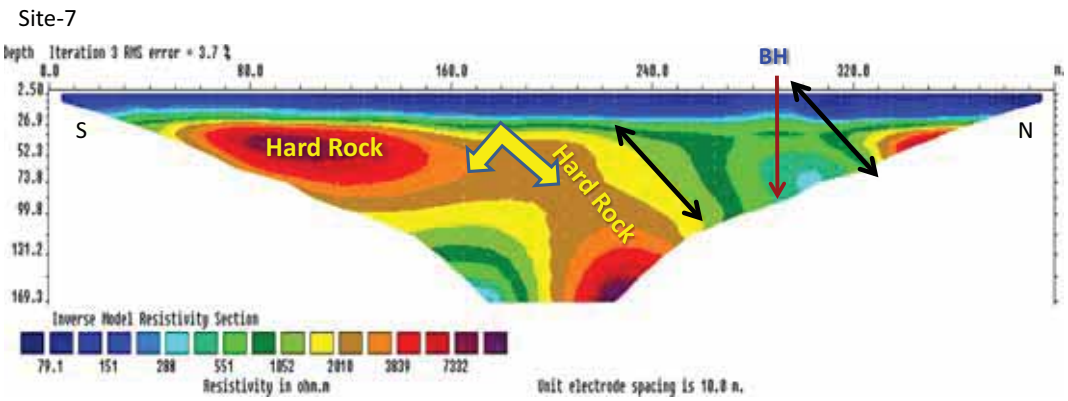

Figure 5. Shows the 2D inverted resistivity model where the northern side of the resistivity section shows more prospects for groundwater exploration as compared to the southern side at site no. 7.

which is inferred as weathered rock formation (figure 5). The inverted resistivity section delineated a high resistivity >4000 Ωm formation sitting at a depth of 50 m in S–N direction and a similar high resistivity body revealed at 169 m depth from the center towards northern side of the section at the deepest depth where there is no prospect for groundwater exploration.

5.1.4 *Site-8 (Block-B)*

The 2D inverted resistivity model at site-8 is laid in SE–NW direction with a lateral coverage of 800 m on the ground and this model resistivity section shows the resistivity structure as well as hydrogeological scenario of the subsurface geological formation up to a depth of 230 m (figure 6). The near

surface layer shows a highly weathered rock formation up to a depth of 15 m. It revealed a prospect groundwater scenario lying below 320 m lateral distance at a depth of around 100 m, which is sandwiched between the two high resistivity layers (figure 6). The low resistivity contrast zone is the prospect groundwater zone and it appears to be connected to the near surface layer towards SE as well as in NW directions (figure 6). Towards the NW side, a very high resistivity and tectonically deformed type of geological structure/feature was delineated from deepest up to ∼40 m depth.

5.1.5 *Site-12 (Block-B)*

The 2D inverted resistivity section at site-12 located in block-B is laid in S–N direction. It revealed a large variation in the subsurface resistivity of the geological formation (figure 7). The resistivity of the formation ranges from <65 to >38,400 Ωm showing a wide range of variation in resistivity within the entire resistivity section (figure 7). The model resistivity section shows a clear-cut groundwater prospect zone between 50 and 70 m depth between lateral distance 160 m and 240 m (figure 7). The inverted model clearly delineated the high resistivity tectonically deformed geological structure from the deeper depth at 170 m to a shallower 50 m depth in the north direction, while in southern side there is totally a different geoelectric structure with a resistivity ∼6500 Ωm zone at a depth of 27 m is revealed from the section (figure 7).

5.1.6 *Site-15 (Block-D)*

The 2D inverted resistivity section at site-15 is located in block-D and is laid in S–N direction. The model resistivity section shows a layered resistivity structure up to a depth of ∼27 m (figure 8). It revealed a clear-cut high and low resistivity formation from 70 m to bottom 170 m depth almost

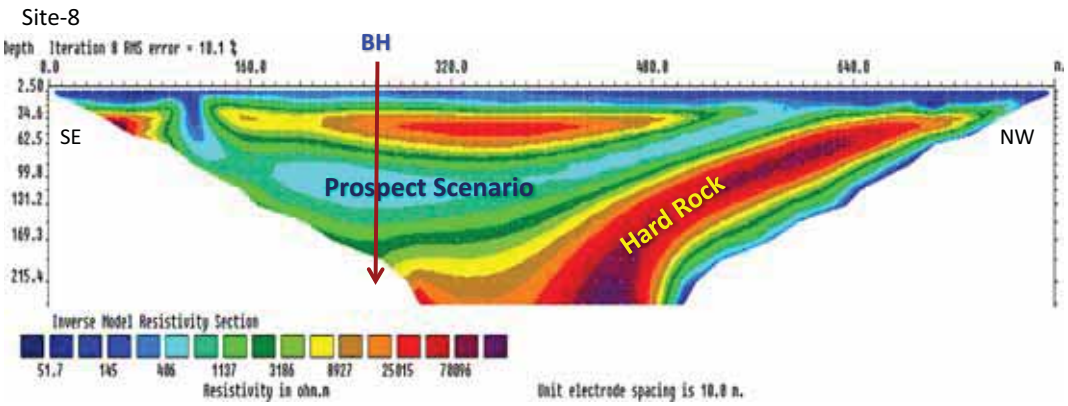

Figure 6. Depicted the 2D inverted resistivity model with clear-cut delineation of high resistivity geological structure inclined towards NW and a prospect groundwater zone sandwiched between high resistivity rock mass at site no. 8.

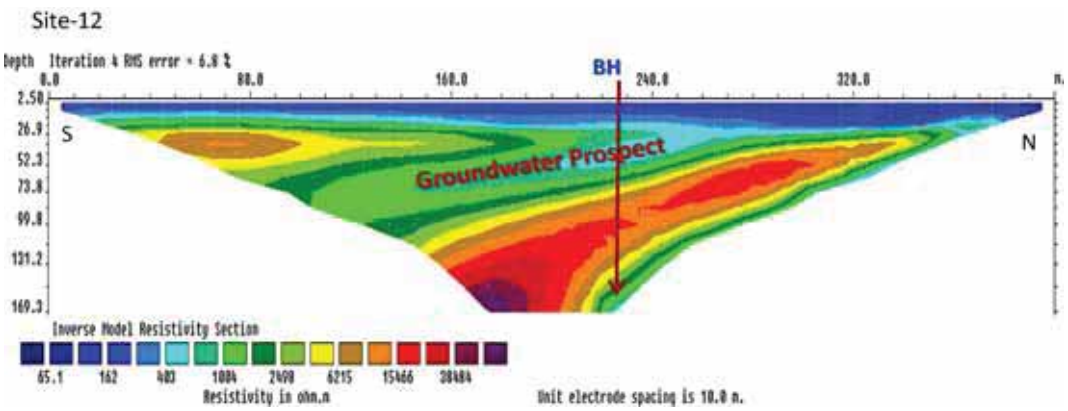

Figure 7. Depicted the 2D inverted resistivity model with a large resistivity contrast of the geological formation and delineated prospect groundwater zone between 50 and 70 m depth lying within the lateral distance 160 and 240 m at site no. 12.

in the center of the resistivity section and demarcated the high resistivity geological structure (figure 8). Well developed resistivity contrast between the high and low resistivity geological formation in the center of the section is inferred as the fault zone (**F–F**), which separated the high and low resistivity zones at the contact of the fault zone as shown in figure 8. The resistivity contrast developed between these geological formations is of the order of ∼66,800 **Ω**m, which is very high and depicts that one side of the fault is very resistive and the other side is very conductive, which is delineated at a depth of 70–170 m (figure 8). This contact of the high and low resistivity zone is the main potential target for groundwater exploration and development in the present geological setting.

6. Characteristics resistivity for various geological formations

From the overall study, analysis and interpretation of the resistivity dataset achieved in the study area, the characteristic resistivity for the various geological formations was estimated based on the inverted resistivity results. Table 1 shows the

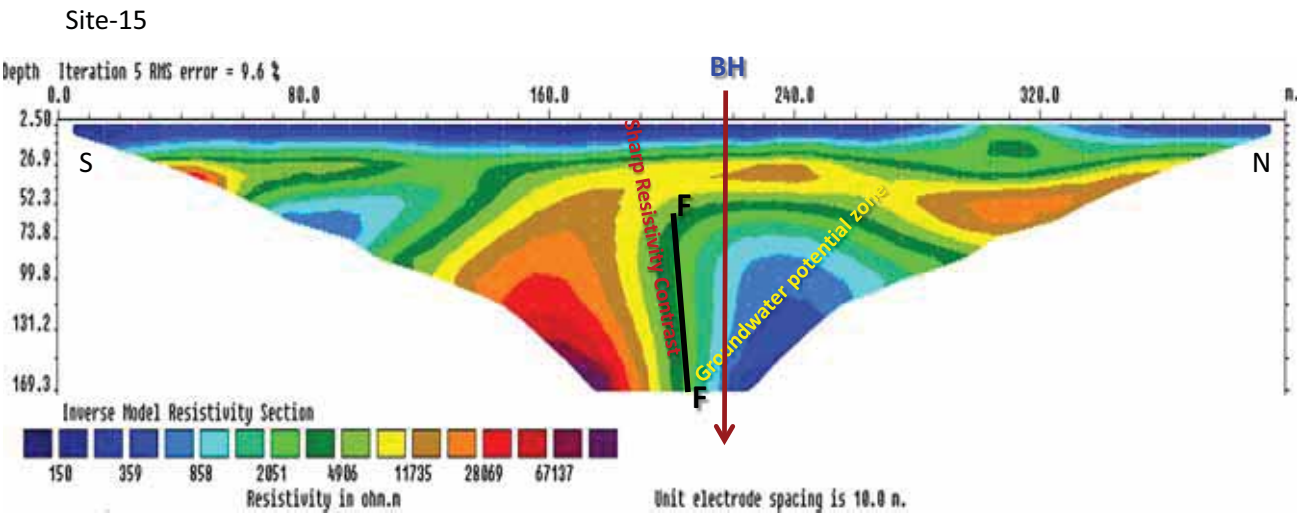

Figure 8. Shows the 2D inverted resistivity model which revealed a high and a low resistivity geological formation, which is inferred as the fault (**F–F**) with a prospect groundwater zone towards the right of the fault at site no. 15.

Table 1. *Characteristics resistivity range of the various geological formations inferred from the 2D modelled resistivity results and the evaluation of groundwater prospect scenario.*

Site no.	Weathered zone (Ωm)	Fractured zone (Ωm)	Saturated weathered/ fractured zone (Ωm)	Massive formation (Ωm)	Groundwater prospect/ aquifer health
1	25–100	250–600	80–350	>5000	Good
2	75–150	190–300	25–250	3900–26,000	Less to moderate
3	300–400	650–800	50–1000	10,000–65,000	Poor
4	230–550	800–1300	100–250	5000–97,500	Moderate
5	100–170	400–700	250–350	>4000	Good
6	150–250	270–380	50–150	2500–3500	Poor
7	50–150	250–350	150–300	>2000	Very good
8	20–50	140–250	30–200	>6000	Good
9	50–250	300–500	50–500	2300–9000	Poor to moderate
10	150–250	300–450	75–400	>6000	Poor
11	150–275	275–550	80–450	>7500	Poor
12	120–175	300–700	25–500	6000–40,000	Good
13	150–250	300–600	75–600	6500–10,000	Poor to moderate
14	60–175	200–800	10–750	>400,000	Poor
15	120–160	250–400	<300	>5000	Very good
16	150–200	200–400	<400	>6500	Moderate to good

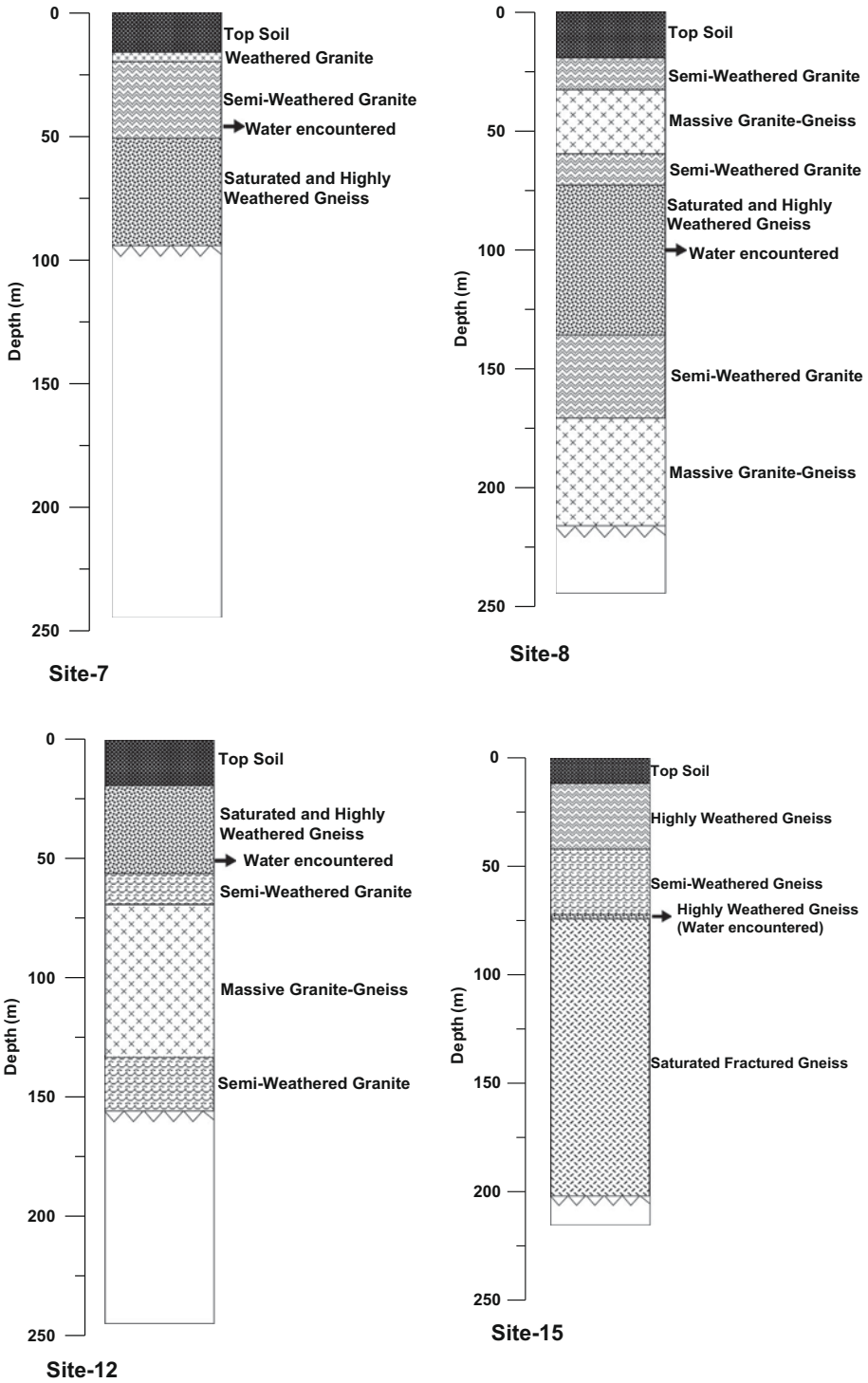

Figure 9. Detailed lithology of the drilled boreholes namely at sites 7, 8, 12 and 15 and its validation showing the water encountered at semi-weathered granite, saturated and highly weathered gneiss and highly weathered gneiss of the granite-gneiss hard rock aquifer system.

detailed information of the various geological formations with their characteristics resistivity range, which was assigned to each of the formations. This table depicted that there is a large variation in the resistivity range for the saturated weathered/fractured zone and the massive formations as well as evaluated the groundwater prospect scenario at each of the sites. This emphasizes that the aquifer zone depends on the nature and amount of fractured and fissured rock mass within the subsurface rock strata as well as their connectivity to the recharge source, which

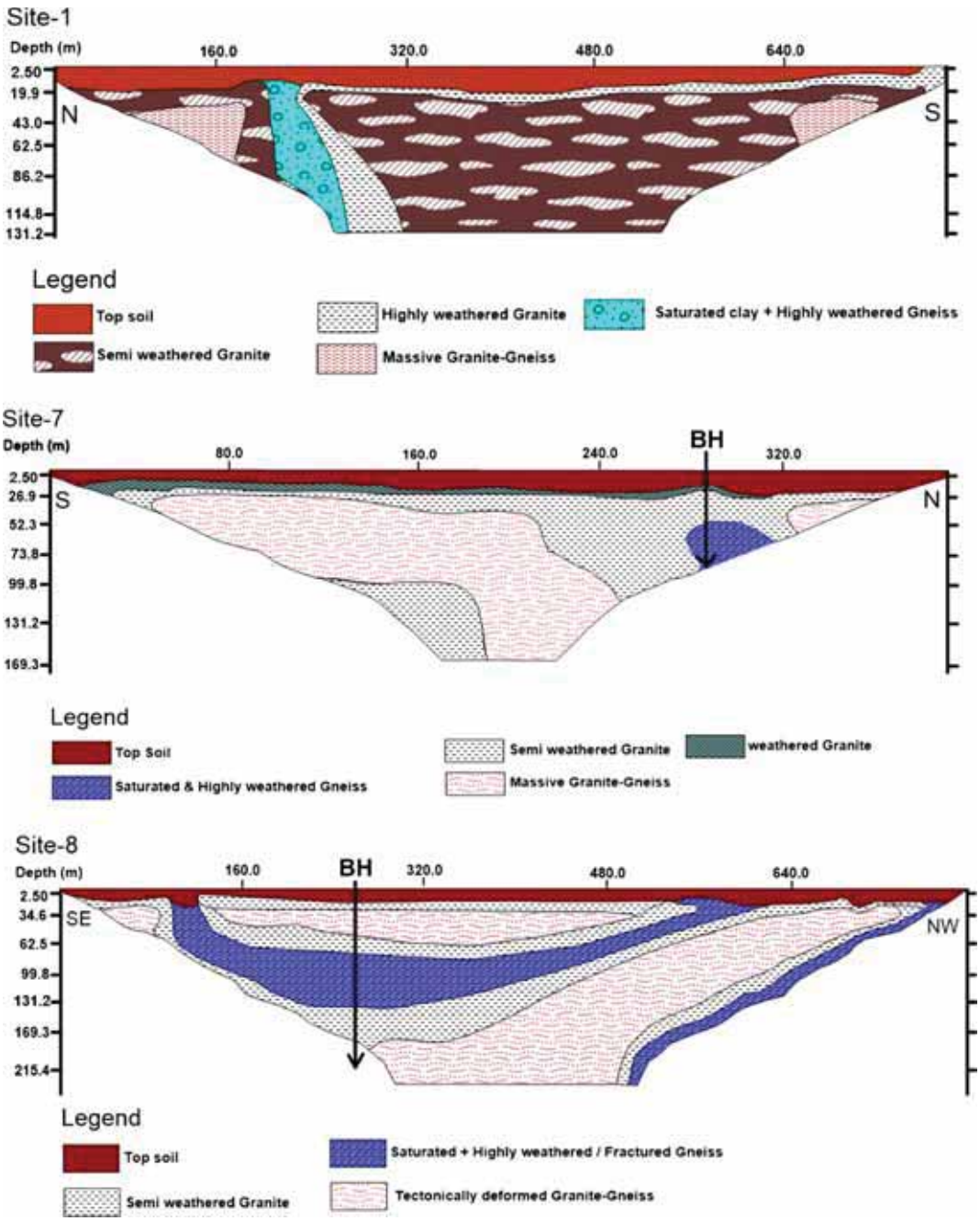

Figure 10. Depicted the conceptual geological models at sites-1, 7, 8, 12 and 15 arrived based on the 2D resistivity results, borehole lithology data and the geological setting of the Chhotanagpur granite-gneiss of Chhotanagpur Gneissic Complex (CGC) region.

ultimately contribute to the groundwater table in an aquifer.

7. Borehole drilling and validation of model results

The new borehole was drilled at four recommended and anomalous sites namely at 7, 8, 12 and 15 considering the favourable resistivity variation, hydrogeological scenario for groundwater availability as well as seeing the resistive and conductive geological setup and their structural nature of the hard rock formation. The modelled resistivity values and the contrast serve as the main guiding principle in deciding and pin pointing the drilling location in all the four unique subsurface geological and structural set up in the varied hard rock terrain. The characteristic of fractured zone as well as saturated weathered/fracture zone as inferred from the resistivity section was different in all these four sites (table 1), which is the main

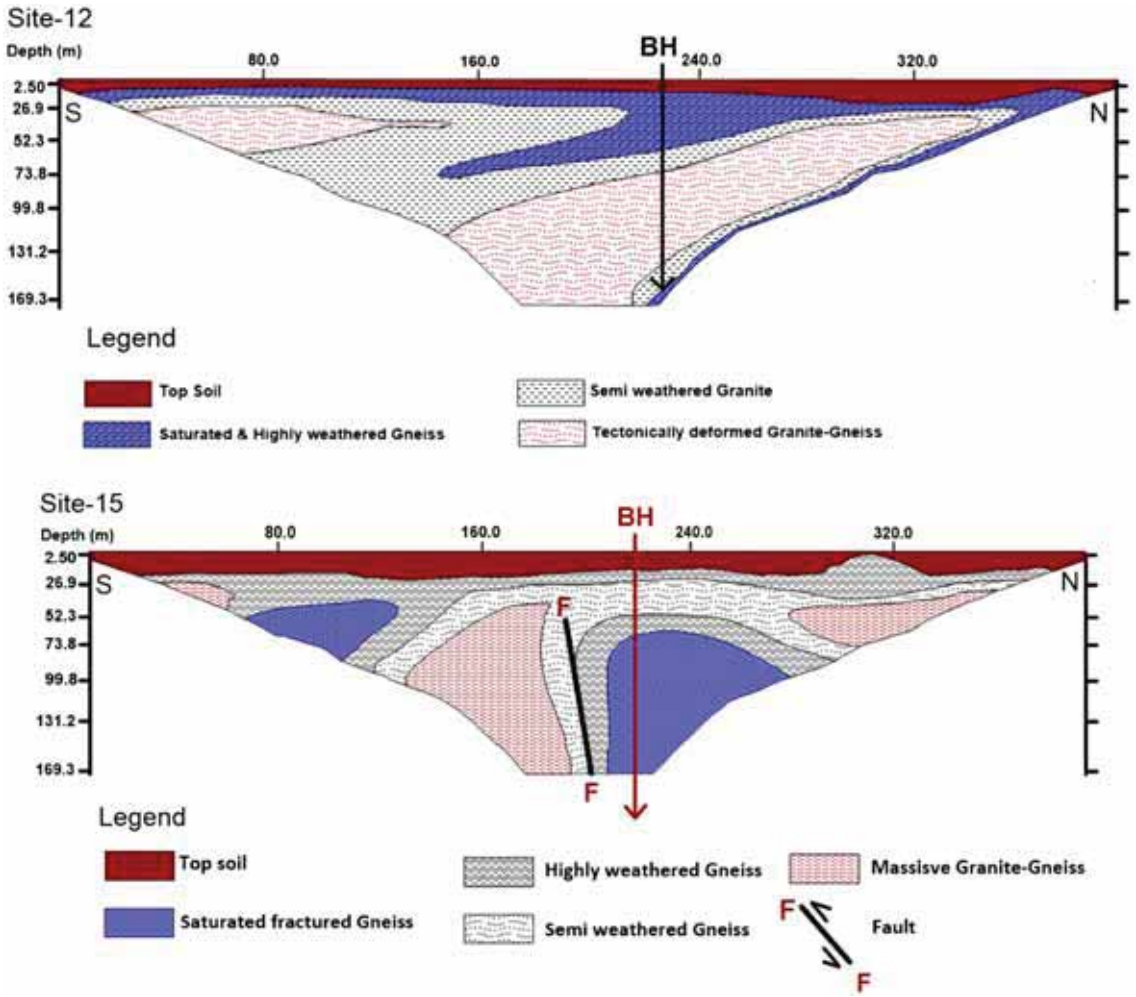

Figure 10. (*Continued.*)

prospect for aquifer in the present geological scenario. All these four sites were drilled as recommended in terms of location as well as their depths and thus validated the electrical resistivity models and the geophysical anomalies for groundwater prospect scenario. These borehole sites encountered saturated fracture(s) and tapped the aquifer zones in the subsurface rock strata both at the shallower (<70 m) and at the deeper depths (100 to ≥150 m) of the geological strata (figure 9). The yields of these four boreholes vary from 2.00 to 4.25 inch, which is equivalent to 5632–63,769 l/hr of groundwater exploitation and was considered moderate to very good production borehole in the present geological setting.

8. Conceptual geological models

The geological models were derived with the help of 2D electrical resistivity tomography models, geological and hydrogeological information and the borehole lithology data. The conceptual geological models at sites 1, 7, 8, 12 and 15 are prepared and presented here (figure 10). The main unique geological strata encountered in drilling vis-à-vis with the resistivity results from these sites are top soil cover, weathered granite, semi-weathered granite, semi-weathered gneiss, highly weathered granite, highly weathered gneiss, saturated and highly weathered gneiss, saturated fractured gneiss, saturated + highly weathered/fractured gneiss, saturated clay + highly weathered gneiss and massive granite-gneiss (figures 9 and 10). The hydrogeological scenario is revealed both at the shallower between 50 and 70 m depths as well as at the deeper 100 to ≥150 m depths. The hard rock characteristics is quite different at these sites, which was revealed from the drilling rock cuts as well as the characteristic resistivities range achieved for hard rock formations (table 1). The depth to top of the aquifer or the water striking depth varies from 45.6 to 99.9 m depths (figure 9).

Table 2. *Details of the six sites showing groundwater potential target and the recommended depths for drilling along with the yields of the borehole in the study area.*

Site no.	Site name	GPS coordinate	Lateral distance (m) on the ground	Prospect groundwater depth (m)	Resistivity of prospect groundwater zone(s) (Ωm)	Yields of the drilled borehole
1	IIAB-A1	N23°16′4.0″ E85°20′26.6″	Between 190 and 280 m from North	45–150	50–350	Technical problem during drilling
5	IIAB-A5	Between N23°15′52.5″ E85°20′17.3″ and N23°15′46.5″ E85°20′14.7″	Between 240 and 320 m from North	55–140	350–550	Negligible yield
7	IIAB-B7	Between N23°16′22.7″ E85°20′27.4″ and N23°16′29.1″ E85°20′27.7″	Between 240 and 320 m from South	60–100	300–400	4.25 inch
8	IIAB-B8	N23°16′12.9″ E85°20′39.5″ and N23°16′18.1″ E85°20′35.2″	Between 200 and 400 m from SE	90–200	410–450	2.0 inch
12	IIAB-B12	N23°16′21.4″ E85°20′31.3″	Between 200 and 250 m from South	60–170	410–450	2.5 inch
15	IIAB-D15	N23°16′10.4″ E85°20′57.2″ and N23°16′16.5″ E85°20′57.7″	(i) Below 80 m (ii) Between 200 and 260 m from South	(i) 60–100 (ii) 80–200	100–500	3.25 inch

This reflects the disposition of the aquifer is highly variable in the present geological setting and is directly linked to the saturated weathered/fractured zones at various depths. Groundwater is tapped only through the saturated fractured zones in the hard rock system in the present study. The saturated fractured zones within the subsurface were delineated based on the high resolution electrical tomography results, which demarcated the hydrogeological zones for drilling boreholes in order to exploit groundwater resources at different depths. These conceptual geological models along with the borehole lithology results illustrated the detailed geological scenario, hydrogeological variation, amount of groundwater availability and the status of the aquifer in the present hard rock system.

9. Discussion

High resolution geophysical study and the results of the 2D resistivity tomography dataset at 16 sites and their interpretation in terms of hydrogeology revealed the presence of groundwater prospect scenario in and around the study area at different depths with variation in the aquifer zone resistivities. Out of the 16 sites studied only six was considered the most favourable with clear-cut potential groundwater target lying at the shallower to the deeper depths (table 2). The 2D modelled resistivity dataset clearly mapped and delineated the resistivity and conductive geological features and structure(s) of the Chhotanagpur Gneissic Complex (CGC) of the area as well as the basic hard rocks with a wide range of resistivities. The high resistivity of the subsurface geological formation is well delineated, which shows a large resistivity contrast as within the complex geological setting in the study area. As we know in the hard rock system, here in our study the host rock is granite-gneiss. This variety of rock has a large variation in rock physical property (here resistivity) as well as it shows a large anisotropy within a short distance. For example; site-1 and site-5 are located in block-A and are separated from each other at about 225 m away. Also the *in-situ* ground surface condition at site-5 is hard compared to the site-1 as noticed during the geophysical survey, which has resulted in a higher resistivity of top layer at site-5. The high resistivity of the subsurface formations ranges from $\sim$2500 Ωm to a maximum $\sim 3.5 \times 10^5$ Ωm.

Nevertheless, the resistivity of the groundwater prospect zones lies between 50 and 550 Ωm, which depicts the differential weathered and fractured hard rock aquifer system that holds substantial amount of water within the weathered–fractured rock matrix. Based on the 2D resistivity data interpretation, model results and the yields of the drilled boreholes, it was found that the block-B has more potentiality for groundwater development as compared to block-A and D of the area. The details of the groundwater potential sites recommended for borehole drilling for exploration and development of groundwater resources is given in table 2. The borehole drilling was successfully completed at the anomalous sites 7, 8, 12 and 15 as given in table 2 and are now used for groundwater exploitation and development in the study area. It was noticed that the borehole drilling at site-1 was not completed due to a technical problem of the drilling rig as it encounters sticky and muddy type of clay formation at the near surface layers to about 25 m depth, which makes it very difficult for the drilling rig to penetrate down the earth. While at site-5, the borehole has produced a negligible yield of water. These two boreholes (viz., sites 1 and 5) were not used for further exploitation and groundwater development in this area. In addition, the hydrogeological investigation was carried out in and around the study area in order to know the water table variation as well as the availability of groundwater. The water level was measured from five open large diameter dugwells including one borehole. It was found that the static water level varies from 5.25 to 8.05 m below ground level (bgl), which suggests the shallow water table of the groundwater in the area. It is confirmed from the study that the main aquifer(s) is trapped within the hard rock system at a shallower between 50 and 70 m depths as well as between 100 and ≥150 m at a deeper depths, which is under the confined condition with a large pressure within the aquifer system (figures 9 and 10). Nevertheless, the shallow static water table as well as the different yield values of the boreholes (table 2) guided that there is a substantial rainfall recharge to the aquifer system in the study area. But the matter of delineating the aquifer zone(s), saturated fractured zone(s) in the granite-gneiss hard rock region of the Chhotanagpur Gneissic Complex terrain and pin pointing the drilling borehole location for a productive water well in this diverse geological set-up is a challenging and critical task for the groundwater scientists.

10. Conclusions

The close look of the inverted 2D high resolution resistivity datasets shows a large resistivity variation ∼2500 Ωm to a maximum ∼3.5×10^5 Ωm within the three blocks, viz., A, B and D of the studied area in the complex hard rock geological terrain. This suggests different degree of weathering, fracturing and saturated weathered/fractured part of the rocks in the hard rock aquifer system of the plateau region in Chhotanagpur Gneissic Complex region. The resistivity tomography results do clearly mapped the massive rock, structural feature and the hydrogeological zones within the subsurface at different depths between ∼30 and 220 m. The geophysical inversion of the 2D resistivity dataset revealed the groundwater prospect scenario at six sites based on the substantial resistivity contrast between the highly weathered/fractured and the saturated rocks with respect to the massive rocks, which mostly lies at a deeper depth ≥100 m as groundwater availability at shallower depths <100 m is a meager. The low resistivity inferred as the prospect groundwater zone(s) signifies favourable hydrogeological scenario lies below the hard rock formation and also between two high resistivity rocks is situated under the confined condition, which are the potential target(s) for groundwater exploration and development. The interpretation of 2D models clearly shows the average resistivity of the aquifer zone lies in the range of ∼50 to around 500 Ωm and is validated and correlated from the lithology data from the borehole drilling results. Nevertheless, the broad resistivity range between 10 and 1000 Ωm inferred from the model results, which represented the saturated weathered/fractured granite-gneiss rocks. This interpretation highlights the availability of groundwater resources is more prone where the rocks are highly weathered/fractured and at the same time such formations was connected with the saturated fracture(s)/deep fracture to the recharge source in this area. The drilling was confirmed and validated at four borehole sites from a minimum 94 m to a maximum 215 m depths with their yields ranging from 2.0 to 4.25 inch, which is equivalent to 5632–63,769 l/hr of exploitation and development of groundwater resources. This clearly indicates the large variation in amount of water availability within the differential weathered and fractured rock matrix of the Chhotanagpur Gneissic Complex. However, the conceptual geological models aided in detailed understanding of

the geological setting, hydrogeological variation, groundwater availability and the status as well as depths of the aquifer in the present hard rock aquifer system. The present study illustrated the hydrogeology, the useful characteristic resistivities as well as the productive boreholes in the hard rock granite-gneiss aquifer system of the studied area, delineated the aquifer(s) zones and pin pointed the drilling location of boreholes for sustainable groundwater exploration and development in the complex geological setting of Chhotanagpur Gneissic Complex of Ranchi area.

Acknowledgements

Authors are grateful to Dr V M Tiwari, Director, CSIR–National Geophysical Research Institute, Hyderabad, India, for his kind permission and encouragement for publishing the scientific work and results on exploration and prospecting for groundwater resources. We are thankful to Dr R Ramani, former Director IIAB, Ranchi and ICAR New Delhi for financial support of the project activity and the necessary logistics during the geophysical field investigations. We acknowledged the kind help of Drs Nirmal Kumar, Vijai Pal Bhadana, N K Sinha and Birendra Kumar Yadav of IIAB Ranchi for execution of the project activity, their valuable interactions, discussion about the area and the problem of groundwater. I am very much thankful to Dr Vijai Pal Bhadana for taking keen interest for successfully completing the borehole drilling activity of the project. First author thanks Dr S Thiagarajan for drawing and making the lithology of the drilled boreholes. The CSIR-NGRI reference number of the manuscript is NGRI/Lib/2019/Pub-84. Crucial comments and suggestions by the anonymous reviewer had significantly improved the quality of the paper. The Funding was provided by IIAB Ranchi, Jharkhand (Grant Number IIAB/OSD/04/2015/8046).

References

ABEM 2012 ABEM Instruction Manual – Terrameter LS; 110p.

Adepelumi A A, Yi M J, Kim J H, Ako B D and Son J S 2006 Integration of surface geophysical methods for fracture detection in crystalline bedrocks of southwestern Nigeria; *Hydrogeol. J.* **14** 1284–1306.

Andrade R 2011 Intervention of electrical resistance tomography (ERT) in resolving hydrological problems of a semi-arid granite terrain of southern India; *J. Geol. Soc. India* **78(4)** 337–344.

Baidya T K 2015 Archean metallogeny and crustal evolution in the East Indian Shield; *Earth Sci.* **4(4–1)** 1–14, https://doi.org/10.11648/j.earth.s.2015040401.11.

Batayneh Awni T 2001 Resistivity imaging for near-surface resistive dyke using two-dimensional DC resistivity techniques; *J. Appl. Geophys.* **48** 25–32.

Colella A, Lapenna V and Rizzo E 2004 High-resolution imaging of the High Agri Valley Basin (southern Italy) with electrical resistivity tomography; *Tectonophys.* **386** 29–40.

Dahlin T 1996 2-D resistivity surveying for environmental and engineering applications; *First Break* **14** 275–283.

Demanet D, Pirard E, Renardy F and Jongmans D 2001 Application and processing of geophysical images for mapping faults; *Comput. Geosci.* **27** 1031–1037.

Dahlin T and Loke M H 1998 Resolution of 2D Wenner resistivity imaging as assessed by numerical modelling; *J. Appl. Geophys.* **38** 237–249.

Griffiths D H, Turnbull J and Olayinka A I 1990 Two-dimensional resistivity mapping with a computer controlled array; *First Break* **8** 121–129.

Griffiths D H and Barker R D 1993 Two-dimensional resistivity imaging and modeling in areas of complex geology; *J. Appl. Geophys.* **29** 211–226.

Gupta G, Patil J D, Maiti S, Erram V C, Pawar N J, Mahajan S H and Suryawanshi R A 2015 Electrical resistivity imaging for aquifer mapping over Chikotra basin, Kolhapur district, Maharashtra; *Environ. Earth Sci.* **73** 8125–8143.

Hossain D 2000 2D Electrical imaging survey in hydrogeology, the Bangladesh; *J. Sedim. Res.* **18(1)** 57–66.

Kumar D 2004 Conceptualization and optimal data requirement in simulating flow in weathered-fractured aquifers for groundwater management; Ph.D. Thesis, Osmania University, Hyderabad, 213p.

Kumar D, Rao V A, Nagaiah E, Raju P K, Mallesh D, Ahmeduddin M and Ahmed S 2010 Integrated geophysical study to decipher potential groundwater and zeolite-bearing zones in Deccan Traps; *Curr. Sci.* **98(6)** 803–814.

Kumar D 2012 Efficacy of electrical resistivity tomography technique in mapping shallow subsurface anomaly; *J. Geol. Soc. India* **80(3)** 304–307.

Kumar D, Rao V A and Sarma V S 2014 Hydrogeological and geophysical study for deeper groundwater resource in quartzitic hard rock ridge region from 2D resistivity data; *J. Earth Syst. Sci.* **123(3)** 531–543.

Kumar D, Mondal S, Nanda M J, Harini P, Soma Sekhar B M V and Sen M K 2016a Two-dimensional electrical resistivity tomography (ERT) and time domain induced polarization (TDIP) study in hard rock for groundwater investigation: A case study at Choutuppal Telangana, India; *Arab. J. Geosci.* **9(5)** 1–15, https://doi.org/10.1007/s12517-016-2382-1.

Kumar D, Mondal S, Soma Sekhar B M V, Balaji T, Nandan M J and Rangarajan R 2016b Full waveform inversion of 2D resistivity and IP data for groundwater exploration in granite aquifers: Implication for complex tectonical setting; *J. Appl. Hydrol.* **XXIX(1–4)** 9–19.

Kumar D, Mondal S, Rajesh K and Rangarajan R 2015 Mapping shallow subsurface hard and soft rock structure

in complex geological terrain for groundwater prospecting and exploitation in Anantapur District, Andhra Pradesh; Abstract volume in 52nd Annual Convention and meeting of IGU on 'Near Surface Earth System Sciences' held during 3–5 November, 2015 at NCAOR Goa, India, 10p.

Kumar D, Subba Rao D V, Mondal S, Sridhar K, Rajesh K and Satyanarayanan M 2017 Gold-sulphide mineralization in ultramafic–mafic–granite complex of Jashpur, Bastar Craton, Central India: Evidences from geophysical studies; *J. Geol. Soc. India* **90(2)** 147–153, https://doi.org/10.1007/s12594-017-0692-x.

Loke M H and Barker R D 1996 Rapid least-squares inversion of apparent resistivity pseudosections by a quasi-Newton Method; *Geophys. Prospect.* **44(1)** 131–152.

Loke M H and Dahlin T 2002 A comparison of the Gauss–Newton and quasi-Newton methods in resistivity imaging inversion; *J. Appl. Geophys.* **49** 149–162.

Loke M H 1997 Electrical imaging surveys for environmental and engineering studies: A practical guide to 2-D and 3-D surveys, 61p.

Loke M H 2012a 2D and 3D resistivity/IP inversion and forward modeling, Geotomo Software Penang, Malaysia.

Loke M H 2012b Tutorial: 2D and 3D electrical imaging surveys; 172p.

Radhakrishna B P 1952 Mysore Plateau: Its structural and physiographic evolution; *Bull. Mysore Geologists Assoc.,* No. 3.

Radhakrishna B P 1993 Neogene uplift and geomorphic rejuvenation of Indian Peninsula; *Curr. Sci.* **64** 787–793.

Robert T, Dassargues A, Brouyère S, Kaufmann O, Hallet V and Nguyen F 2011 Assessing the contribution of electrical resistivity tomography (ERT) and self-potential (SP) methods for a water well drilling program in fractured/karstified limestones; *J. Appl. Geophys.* **75** 42–53.

Sasaki Y 1992 Resolution of resistivity tomography inferred from numerical simulation; *Geophys. Prospect.* **40** 453–464.

Singh S P and Verma R A K 2015 Water resource management in a hard rock terrain for sustaining irrigated agriculture – A case study of Jharkhand, India; *Int. J. Environ. Sci. Dev.* **6(10)** 795–798.

Singh T B N 2013 Groundwater information booklet, Ranchi district, Jharkhand – Central Groundwater Board (CGWB), Ministry of Water Resources, Govt. of India, State Unit Office Ranchi, Mid-Eastern Region, Patna, 27p.

Steeples D W 2001 Engineering and environmental geophysics at the millennium; *Geophysics* **66(1)** 31–35.

Suzuki K, Toda S, Kusunoky K, Fujimitsu Y, Mogi T and Jomori A 2000 Case studies of electrical and electromagnetic methods applied to mapping active faults beneath the tick Quaternary; *Eng. Geol.* **56** 29–45.

Thiagarajan S, Rai S N, Kumar D and Manglik A 2018 Delineation of groundwater resources using electrical resistivity tomography; *Arab. J. Geosci.* **11(9)** 1–16, https://doi.org/10.1007/s12517-018-3562-y.

Corresponding editor: Arkoprovo Biswas